Available online at www.sciencedirect.com
ScienceDirect
Carbohydrate Research 342 (2007) 2404–2415
Carbohydrate RESEARCH

Exopolysaccharides produced by *Inquilinus limosus*, a new pathogen of cystic fibrosis patients: novel structures with usual components

Yury Herasimenka,[a,†] Paola Cescutti,[a,*] Giuseppe Impallomeni[b] and Roberto Rizzo[a]

[a]*Dipartimento di Biochimica Biofisica e Chimica delle Macromolecole, Università di Trieste, via L. Giorgieri 1, I-34127 Trieste, Italy*
[b]*Istituto di Chimica e Tecnologia dei Polimeri, CNR, Viale A. Doria 6, I-95125 Catania, Italy*

Received 1 June 2007; received in revised form 11 July 2007; accepted 12 July 2007
Available online 21 July 2007

This paper is dedicated to the memory of Dr. William F. Fett (USDA, Wyndmoor, PA, USA), who would have enjoyed participating in this study

Abstract—The major cause of morbidity and mortality in patients with cystic fibrosis, an autosomal recessive disorder, is chronic microbial colonisation of the major airways that leads to exacerbation of pulmonary infection. Several different microbes colonise cystic fibrosis lungs, and *Pseudomonas aeruginosa* is one of the most threatening, since the establishment of mucoid (alginate producing) strains is ultimately associated with the patient's death. Very recently a new bacterium, named *Inquilinus limosus*, was repeatedly found infecting the respiratory tract of cystic fibrosis patients. Its multi-resistance characteristic to antibiotics might result in the spreading of *I. limosus* infection among the cystic fibrosis community, as recently happened with strains of the *Burkholderia cepacia* complex. Since exopolysaccharides are recognised as important virulence factors in lung infections, the primary structure of the polysaccharide produced by *I. limosus* strain LMG 20952^T was investigated as the first step in understanding its role in pathogenesis.
The structure was determined by means of methylation analysis, acid degradations, mass spectrometry and NMR spectroscopy. The results showed that the bacterium produced a mixture constituted of the following polymers:

[3)-[4,6-*O*-(1-carboxyethylidene)]-β-D-Glc*p*(1→]$_n$

[2)-[4,6-*O*-(1-carboxyethylidene)]-α-D-Man*p*(1→]$_n$

Both polymers were completely substituted with pyruvyl ketal groups, a novel structural characteristic not previously found in bacterial polysaccharides. The absolute configuration of all pyruvyl groups was *S*. Inspection of possible local conformations assumed by the two polysaccharide chains showed features, which might provide interesting clues for understanding structure–function relationships.

Keywords: Exopolysaccharide; *Inquilinus limosus*; Cystic fibrosis; Structure; NMR; ESIMS

Abbreviations: AMP, antimicrobial peptides; BCC, *Burkholderia cepacia* complex; CF, cystic fibrosis; CPS, capsular polysaccharides; EPS, exopolysaccharides; YEM, yeast extract-mannitol medium

* Corresponding author. Tel.: +39 040 5583685; fax: +39 040 5583691; e-mail: pcescutti@units.it
† Present address: Yury Herasimenka, FB Biologie/Chemie, Universität Osnabrück, Barbarastr. 11, D-49076 Osnabrück, Germany.

0008-6215/$ - see front matter © 2007 Elsevier Ltd. All rights reserved.
doi:10.1016/j.carres.2007.07.012

1. Introduction

Cystic fibrosis (CF) is an autosomal recessive disorder[1] caused by mutations of the gene coding for the CF transmembrane conductance regulator. This causes the production of very viscous mucus and abnormal electrolyte transport across epithelial cells membranes, resulting in impaired functioning of the respiratory tract and pancreas. The chronic microbial colonisation of the respiratory tract, accompanied by pulmonary infections, is the major cause of death in CF patients. *Pseudomonas aeruginosa*, *Staphylococcus aureus*, *Haemophilus influenzae* and microorganisms of the *Burkholderia cepacia* complex (BCC) are typical pathogens of CF patients. Other microbes, like *Ralstonia pickettii*, *Alcaligenes xilosoxidant*, *Stenotrophomonas maltophilia* and *Burkholderia gladioli* have also been isolated from respiratory samples of CF patients. A new bacterial species, named *Inquilinus limosus*, was recovered from eight CF patients in the USA.[2] It was recently also isolated from German[3] and French[4] CF patients.

I. limosus is a Gram negative species belonging to the α-proteobacteria and thus is not closely related to the principal CF lung infecting bacteria.[2] The full pathogenic potential of *I. limosus* is yet to be determined, however , it may represent a new threat to CF patients as it has: (i) a mucoid phenotype; (ii) multi-resistance to a wide number of antibiotics and; (iii) the ability to persist in the respiratory tract.[3,4] The term 'limosus', meaning full of slime, attracted interest, because the slimy character of bacterial colonies is associated with the production of copious amounts of exopolysaccharides (EPS). The biological role of EPS in CF lung infections has been elucidated for alginate, the polymer produced by *P. aeruginosa*, and its importance to the pathogenesis of the organism demonstrated.[5,6] The roles proposed for alginate in CF infections include inhibition of phagocytosis, hypochlorite scavenging, quenching of reactive oxygen intermediates, interference with opsonisation and suppression of neutrophil chemotaxis. Preliminary studies for cepacian, the EPS produced by the majority of the BCC organisms,[7] have shown its role in inhibiting neutrophils chemotaxis and in scavenging reactive oxygen species.[8] Other investigations have shown that the free hydroxyl groups present on the EPS might form covalent ester bonds with the C3 complement factor,[9,10] and so interfere with the cascade of events leading to complement activation and final bacterial cell lysis. Negatively charged groups (uronic acid, phosphate esters, pyruvate substituents) frequently occurring in bacterial EPS, were associated with inactivation of the host innate immune system through interactions with antimicrobial peptides[11] (AMP).

This study of the chemical structure of the EPS produced by *I. limosus* strain LMG 20952^T, constitutes the first step towards understanding its role in pulmonary infections. Comparison with other polysaccharides involved in CF pulmonary infections, could indicate which structural features are important for the biological activity observed.

2. Experimental

2.1. Bacterial growth and EPS purification

I. limosus strain LMG 20952^T was grown for 72 h at 37 °C on solid yeast extract-mannitol (YEM)[12] medium (2 g yeast extract, 20 g mannitol, 15 g bacto agar per litre of water). Bacterial cells were collected by washing each plate with about 5 mL of 0.9% NaCl. Phenol was added to a final concentration of 5% and the slurry was mixed at 4 °C for 5 h. The cells were removed by centrifugation; the supernatant was precipitated with 4 vol of acetone, and subsequently dissolved in water. This procedure was repeated twice. The EPS solution was dialysed, neutralised and recovered by lyophilisation. Two different batches were obtained and were named **IL4** (400 mg) and **IL5** (957 mg). The average yield was 8 mg EPS/Petri dish for **IL4** and 15 mg EPS/Petri dish for **IL5**.

2.2. Analytical procedures

Analytical GLC was performed on a Perkin Elmer Autosystem XL gas chromatograph equipped with a flame ionisation detector and an SP2330 capillary column (Supelco, 30 m), using He as the carrier gas. The following temperature programs were used: for alditol acetates, 200–245 °C at 4 °C/min; for methylated alditol acetates, 150–250 °C at 4 °C/min. Separation of the trimethylsilylated (+)-2-butyl glycosides was obtained on a HP1 column (Hewlett–Packard, 50 m), using the following temperature program: 135–240 °C at 1 °C/min. GLC–MS analyses were carried out on a Hewlett–Packard 5890 gas chromatograph coupled to a Hewlett–Packard 5971 mass selective detector.

2.3. Composition analysis

Colorimetric reactions were used to determine total sugars,[13] uronic acids[14] and pyruvyl substituents,[15] the latter after hydrolysis of a 0.4% EPS soln with 2 N HCl at 100 °C for 3 h. Hydrolysis was performed with 2 M CF_3COOH: for EPS at 125 °C for 1 h, and for oligosaccharides at 100 °C for 6 h. Alditol acetates were prepared as described[16] using inositol as internal standard. Methanolysis was performed with 1 M HCl in MeOH (Supelco) at 85 °C for 18 h according to Dudman et al.[17] For the determination of the absolute configuration of the sugar residues, a sample of **IL5** was

hydrolysed with 2 M CF_3COOH at 125 °C for 1 h, and subsequently subjected to butanolysis with (+)-2-butanol followed by GLC analysis of the derived trimethylsilylated glycosides.[18,19]

2.4. Linkage analysis

Methylations of polysaccharides were performed as described by Hakomori,[20] but using potassium methylsulfinyl-methanide,[21] while oligosaccharides were methylated according to Dell.[22] The permethylated samples were hydrolysed, derivatised into alditol acetates and analysed by GC–MS. Molar ratio values were corrected by the use of effective carbon-response factors.[23] In some cases, the EPS samples were exchanged to the protonated form at 4 °C (using the resin Amberlite® IR120 H^+-form) and subsequently sonicated at the same temperature prior to the methylation reaction.

2.5. Ozonolysis and separation of the products

EPS **IL5** (100 mg) was dissolved in 0.1 M $NaHCO_3$ and the soln was bubbled with ozone at a flow rate of 3.3 mL/s,[24] for 45 min. The sample was then dialysed, neutralised and freeze-dried. It was separated by size-exclusion chromatography on a Bio-Gel P-10 column (1.6 cm id × 90 cm) equilibrated in 0.05 M $NaNO_3$ at a flow rate of about 6 mL/h. The elution profile showed a peak at V_0 flanked by a large shoulder. Fractions belonging to the shoulder, and therefore characterised by a lower molecular weight, were pooled together, dialysed and recovered by lyophilisation (**IL5-OZ**).

2.6. Ion-exchange chromatography

IL5 sample was subjected to two consecutive ion-exchange chromatographies on a DEAE Sepharose CL-6B (2.5 cm id × 5.5 cm) column. The sample (80.5 mg) was dissolved in 80 mL Tris–HCl 0.05 M, pH 7.5 and applied to the column previously equilibrated in the same buffer. The elution was performed first with the same buffer, followed by two saline gradients: 0–2 M NaCl and 2–3 M NaCl in Tris–HCl 0.05 M, pH 7.5. Finally the column was washed with citrate buffer 0.05 M, pH 3.5, 3 M NaCl. Detection of sugar-containing fractions was performed with the colorimetric test for total carbohydrates.[13] Two peaks were obtained and fractions belonging to the same peak were pooled together, dialysed, neutralised and freeze-dried. The peak enriched in mannose (34.2 mg), as revealed by composition analysis, was subjected to a second ion-exchange chromatography; all the experimental steps were repeated as reported above and a fraction further enriched in mannose was isolated (**IL5-IEC**) (Table 1).

Table 1. Monosaccharide analysis of batches **IL4**, **IL5** and sample **IL5-IEC** from ion-exchange chromatography

Monosaccharide	EPS samples		
	IL4	**IL5**	**IL5-IEC**
Rha	0.03		
Man	3.35	1.31	11.80
Gal	0.10	0.05	0.32
Glc	1.00	1.00	1.00

2.7. Depyruvylation reaction and product recovery

Sample **IL4** (1 g/L) was treated with 0.5 M oxalic acid at 100 °C for 2 h,[25] dialysed, neutralised and recovered by freeze-drying (**IL4-DP**). Sample **IL5** (1 g/L) was treated with 0.5 M oxalic acid at 100 °C for 2 h. Afterwards the solution was cooled, and oxalic acid was precipitated by addition of excess $CaCO_3$ with slight warming. After centrifugation, the supernatant was first dialysed against a small volume of water with two changes, in order to recover the extra-dialysate (**IL5-DPE**); then it was extensively dialysed, neutralised and recovered by freeze-drying (**IL5-DP**). **IL5-DPE** was concentrated and separated by size-exclusion chromatography on a Bio-Gel P-2 column (1.6 cm id × 90 cm) equilibrated in water, and using a differential refractive index detector (WGE Dr. Bures, LabService Analytica). Fractions were collected every 15 min. Selected single fractions were lyophilised and subjected to ESIMS analysis, followed by reduction with $NaBD_4$ and subsequent methylation analysis. **IL5-DP** was subjected to methylation analysis, and 1D and 2D NMR spectroscopy.

2.8. Electrospray mass spectrometry

The mass spectra were recorded on a API-I PE SCIEX quadrupole mass spectrometer equipped with an articulated ion spray and connected to a syringe pump for the injection of the samples. The instrument was calibrated using a polypropylene glycol mixture (3.3×10^{-5} M polypropylene glycol M_n 425, 1×10^{-4} M polypropylene glycol M_n 1000 and 2×10^{-4} M polypropylene glycol M_n 2000), 0.1% MeCN and 2 mM ammonium formate in 50% aq MeOH. The fractions from gel filtration chromatography were dissolved in 200 μL of 50% MeCN in MilliQ water, 0.25 mM ammonium acetate. The spectra were recorded in the positive ion mode, using an injection flow rate of 5 μL/min, with the ionspray voltage at 5000 V and the orifice potential at 50 V, and using a step size of 0.1 amu.

2.9. NMR spectroscopy

Samples, previously sonicated to decrease the molecular weight, were exchanged three times with 99.9% D_2O by lyophilisation and finally dissolved in 0.7 mL 99.96% D_2O. Spectra were acquired at 50 °C on a VARIAN^{UNITY} INOVA spectrometer operating at

500 MHz (^{1}H). 2D experiments were performed using standard VARIAN pulse sequences and pulsed field gradients for coherence selection when appropriate. TOCSY spectra were acquired for each sample with three spin-lock times: 30, 60 and 120 ms. T-ROESY spectra were acquired with a 0.4 s mixing time. Chemical shifts are expressed in ppm using acetone as internal reference (δ_H 2.225 ppm, δ_C 31.07). 1D NMR spectra were analysed using the MestreC software.

2.10. Construction of three-dimensional models of oligosaccharides

Molecular models of α-(1→2)-mannan and β-(1→3)-glucan chains were obtained from the Sweet data base managed by the German Cancer Research Centre Foundation (http://www.dkfz-heidelberg.de/spec/sweet2/) at Heidelberg (Germany). Two oligomers were obtained from the data base: [2)-α-D-Man*p*(1→]$_6$ and [3)-β-D-Glc*p*(1→]$_4$; the pyruvate substituents in the *S* configuration were then added on each sugar residue evaluating the proper atom coordinates from the crystallographic structure of 4,6-*O*-(1-carboxyethylidene)]-β-D-Man[26] (and http://xray.bmc.uu.se/hicup/).

3. Results and discussion

3.1. Bacterial growth and exopolysaccharide production

Five different solid media were exploited for expression of the mucoid phenotype of *I. limosus* strain LMG 20952^T (LB, TSA, YEM, Nutrient Agar, Sucrose rich agar) and two different temperatures (30 °C and 37 °C), and the best results were obtained with YEM medium at 37 °C. The choice of this medium was driven by the knowledge that it stimulates the production of very mucoid colonies of the *B. cepacia* complex bacteria, which are CF opportunistic pathogens as well.

3.2. Exopolysaccharide composition

Colorimetric determination of total sugars and uronic acids on **IL4** sample gave 76% (w/w) and 0.79% (w/w), respectively. For composition analysis, the two EPS batches were hydrolysed, the products converted to alditol acetates and analysed by GLC. The data (Table 1) indicated the presence of mannose and glucose in both samples, but in different molar ratios, together with small amounts of rhamnose and galactose.

The ^{1}H NMR spectra of **IL4** and **IL5** (Fig. 1) showed two main signals in the anomeric protons region at 5.18 and 4.94 ppm, which, considering the molar ratio from the sugar analysis (Table 1), were attributed on the basis of their integration values to H-1 of Man and Glc, respectively. The broader anomeric proton signal of

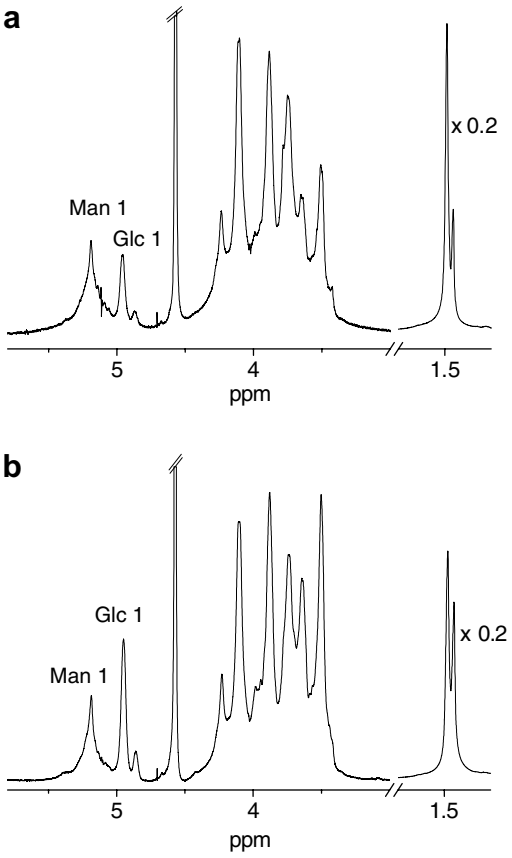

Figure 1. ^{1}H NMR spectra of the native samples **IL4** and **IL5** recorded at 50 °C. ×0.2 indicate that the intensity of the methyl resonances was multiplied by 0.2.

the mannosyl units with respect to that of the glucosyl units might be attributed to the different mobility of the sugar residues. In the high field region of the spectrum, two signals at 1.48 and 1.45 ppm belonging to methyl groups, were in agreement with the presence of pyruvyl substituents, which were attributed, on the basis of their relative integration area with respect to the anomeric proton integrals, to the substituent on mannose and on glucose residues, respectively. The area integration values indicated 100% substitution, a figure in agreement with the results of the colorimetric test for pyruvate (95% molar percentage). ^{13}C NMR and DEPT spectra showed two –CH_3 signals at 25.4 and 25.7 ppm attributed to the pyruvate methyl group, indicating that both pyruvyl substituents were in the *S* absolute configuration.[27] The presence of the ketal substituent was further ascertained by carbonyl signals at 176.2 and 176.0 ppm, and by quaternary carbon signals at 102.7 and 102.4 ppm. Unfortunately, the spectral linewidth of ^{1}H and ^{13}C spectra was quite large, and full assignment through 1D and 2D NMR spectroscopy was not feasible. Glucose and mannose were shown to be in the D absolute configuration by GLC of their chiral alcohol derivatives.[18,19]

3.3. Glycosidic linkage determination of native EPS

Various methylation procedures were performed on **IL4** and **IL5** samples, in the sodium salt as well as in the protonated form. The only reaction, which gave useful results was the one conducted on a sample of **IL5**, previously exchanged to its acidic form and heavily sonicated, both treatments carried out at 4 °C. The analysis showed the presence of 3-substituted glucopyranose, 2-substituted mannopyranose, 3,4,6-trisubstituted glucopyranose, 2,4,6-trisubstituted mannopyranose, and 4-substituted galactopyranose in the molar ratios 0.23:0.37:1.00:0.20:0.07. Methylation analysis data were not stoichiometric in agreement with the ^{1}H NMR data for **IL5**, where a 1:1 ratio between hexoses and pyruvyl groups was found. Therefore, these data gave only indications on the type of inter-residue linkages: the mannose residues were linked at C-2 and the glucose residues at C-3, both residues bearing the pyruvyl groups at C-4 and C-6. The amounts of 3-linked glucose and 2-linked mannose detected might be due to hydrolysis of the pyruvyl ketal groups catalysed by the carboxylic functions obtained after exchanging the sample to its acidic form.

3.4. NMR spectroscopy of IL5

Although the samples were always sonicated to decrease their molecular weight before recording NMR spectra, the resolution achieved was not satisfactory. Therefore, the sample **IL5** was subjected to ozonolysis[24] to reduce the viscosity of the EPS solution and improve the quality of the NMR spectra, without removing the pyruvyl substituents. This choice was dictated primarily by the lack of commercially available endoglycosidases for the polymers investigated and by the acid labile character of the pyruvyl groups. The product obtained was separated on a Bio-Gel P-10 column giving a peak eluting at V_0, and a large shoulder. Fractions belonging to the shoulder, and characterised by a lower molecular weight, were pooled together (**IL5-OZ**) and subjected to NMR spectroscopy. The ^{1}H and ^{13}C NMR spectra (data not shown) showed a considerable improvement in resolution; integration of the anomeric signals in the ^{1}H NMR spectrum indicated that the molar ratios of Man and Glc were identical to those in the native sample. 2D NMR analysis through COSY, TOCSY and HSQC experiments allowed the complete assignment of ^{1}H and ^{13}C resonances (Table 2), except for H-6s of Glc residues. The TOCSY spectrum acquired with a 0.12 s spinlock time is shown in Figure 2. The mannose resonances were traced from H-1 to H-2 and from H-2 up to H-5 because of the small $^{3}J_{1,2}$ typical of mannose, which slows down magnetisation transfer, while the glucose signals were readily assigned from H-1 up to H-5. No magnetisation transfer from H-5 of both mannose and glucose residues to the respective methylene H-6 protons was observed, because of the small $^{3}J_{5-6}$ arising from the pyruvate locked conformation of the C-6 groups.[28] The H-6s of mannose were assigned through a cross-peak in COSY and TOCSY spectra and through the ^{1}H/^{13}C correlations in the HSQC experiment, after comparing similar experiments carried out on a mannose-enriched sample (see Section 3.5). The chemical shift of Man C-2 and Glc C-3 (Table 2) was consistent with the linkage analysis data indicating that Man was 2-linked and that Glc was 3-linked. The T-ROESY spectrum in Figure 3 showed that Man H-1 had Overhauser contact with Man H-2, but not with Man H-3 or Man H-5, giving further indication of the mannose α-anomeric configuration. As expected for a β-Glc, cross-peaks were found between Glc H-1 and H-3 and between Glc H-1 and H-5. The overall data collected and the lack of cross-peaks in the T-ROESY spectrum of Man H-1 or Glc H-1 with any of the protons belonging to the Glc or Man spin systems, respectively, led us to hypothesise the presence of two homopolysaccharides: an α-(1→2)-mannan fully 4,6-pyruvylated and a β-(1→3)-glucan fully 4,6-pyruvylated.

Table 2. ^{1}H and ^{13}C NMR chemical shifts of **IL5-OZ**

Residue	Nucleus	Chemical shift[b] (ppm)					
		1	2	3	4	5	6,6′
α-Man*p*	^{1}H	5.18	4.22	4.10	3.87	3.73	3.93, 3.71
	^{13}C	102.67	78.85	69.01	74.66	65.03	64.91
Pyr[a]	^{1}H	—	—	1.48			
	^{13}C	176.22	102.73	25.73			
β-Glc*p*	^{1}H	4.94	3.63	3.88	3.50	3.50	n.d.
	^{13}C	103.08	74.80	80.51	74.66	66.65	65.05
Pyr[a]	^{1}H	—	—	1.45			
	^{13}C	175.98	102.43	25.39			

[a] Pyr = 1-carboxyethylidene.
[b] Chemical shifts relative to internal acetone (2.225 ppm for ^{1}H and 31.07 ppm for ^{13}C).

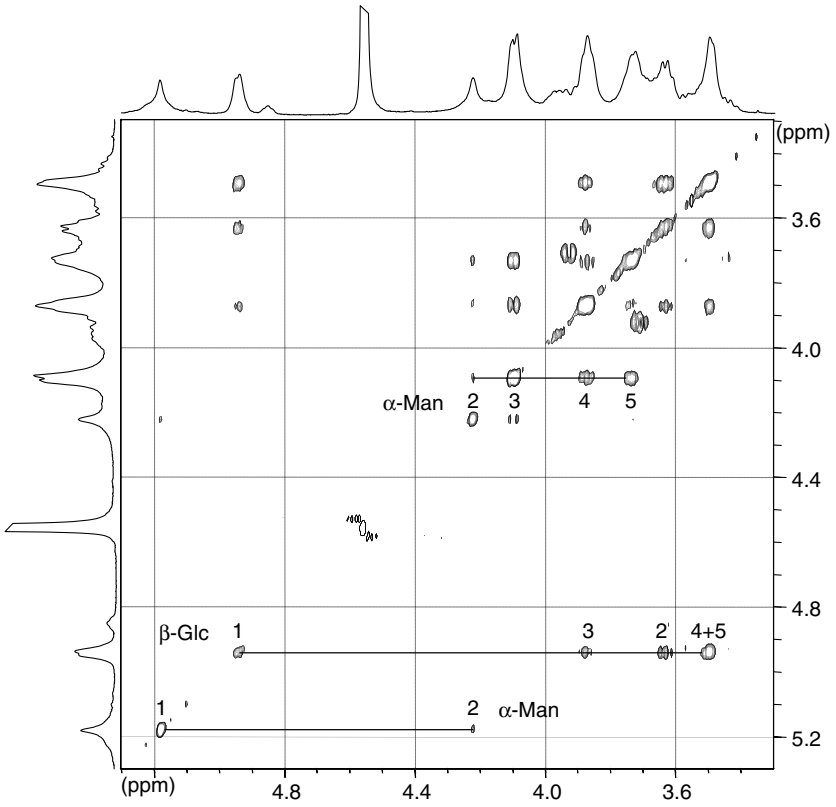

Figure 2. Part of a TOCSY spectrum of the sample **IL5-OZ** recorded at 50 °C and with 0.12 s spin lock time.

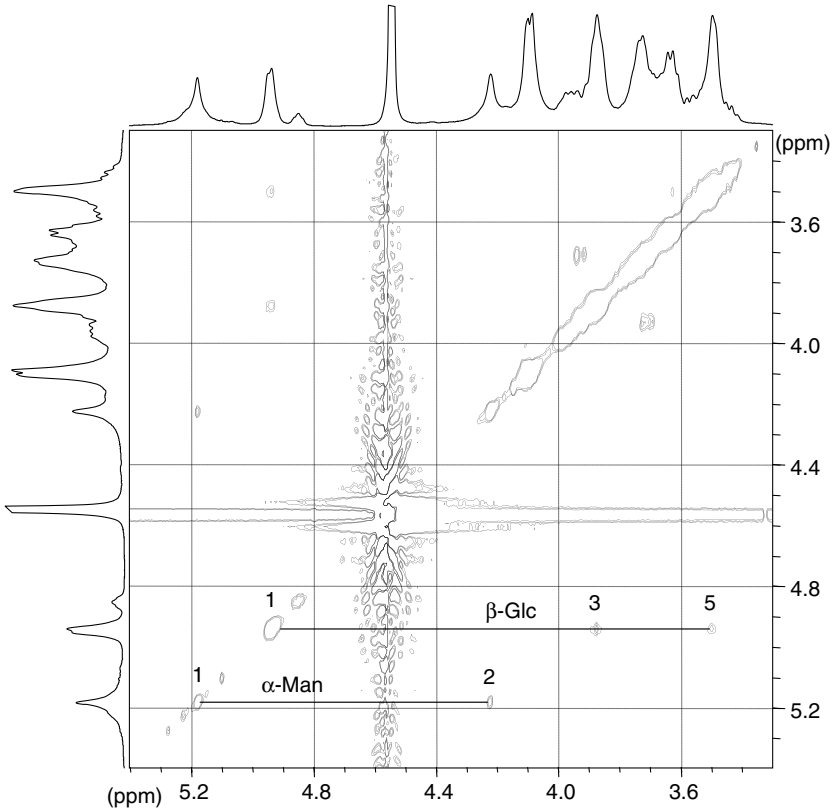

Figure 3. Part of a T-ROESY spectrum of the sample **IL5-OZ** recorded at 50 °C and with a mixing time of 0.4 s.

3.5. Ion-exchange chromatography of IL5 and NMR studies of the products

The sample **IL5** was subjected to two successive separations by ion-exchange chromatography and a fraction enriched in the mannose polymer was isolated (**IL5-IEC**), as revealed by its composition analysis (Table 1). The ^{1}H NMR spectrum of **IL5-IEC** (Fig. 4a) showed a single anomeric resonance at 5.18 ppm, and a single pyruvate methyl signal at 1.48 ppm, suggesting the isolation of a pyruvylated mannan from the **IL5** sample. Similar conclusions were drawn when comparing the ^{13}C NMR spectra of **IL5-IEC** (Fig. 4b) and **IL5-OZ**. COSY, TOCSY and HSQC experiments (data not shown) confirmed the assignments reported in Table 2 for the mannan. A T-ROESY spectrum (data not shown) exhibited an intense correlation between H-1 and H-2 and no correlation between H-1 and H-3 or H-5, confirming an α-1→2) linkage. The isolation of the pyruvylated mannan confirmed the hypothesis that *I. limosus* produced two different EPS: a mannan and a glucan both completely pyruvylated. However, it was not possible to isolate the glucan by ion-exchange chromatography, as all the other peaks in the chromatogram were mixtures of the two polymers.

3.6. Characterisation of the de-pyruvylated exopolysaccharide

IL4 batch was treated with oxalic acid to remove the pyruvyl substituents, the product (**IL4-DP**) was recovered by lyophilisation after dialysis, and an abundant loss of mass, not solely due to the removal of pyruvate, was observed. Composition analysis in terms of alditol acetates of **IL4-DP** gave Man–Glc in the molar ratio 17:1. The ^{1}H and ^{13}C NMR spectra of **IL4-DP** (Fig. 5a and b) showed high intensity anomeric signals at 5.27 and 101.37 ppm, respectively, and others of much lower intensity at 4.79 (^{1}H) and 103.35 (^{13}C) ppm. The ratio between the 5.27 ppm signal intensity and 4.79 ppm signal intensity was 15.3, in agreement with composition analysis data. The most intense anomeric ^{1}H and ^{13}C signals were assigned to an α-mannan, because of the value of 171 Hz[29] measured for the anomeric $^{1}J_{H-C}$ in the proton-coupled ^{13}C spectrum (data not shown), and of the overall hexose composition of the sample. Residual pyruvate signals were detected in the ^{1}H spectrum (at 1.51 ppm) as well as in the ^{13}C spectrum (at 25.55 ppm). The intensity ratio between the mannose anomeric ^{1}H signal and the pyruvate methyl singlet in the ^{1}H spectrum proved that depyruvylation was achieved with a 90% yield. Inspection of the COSY

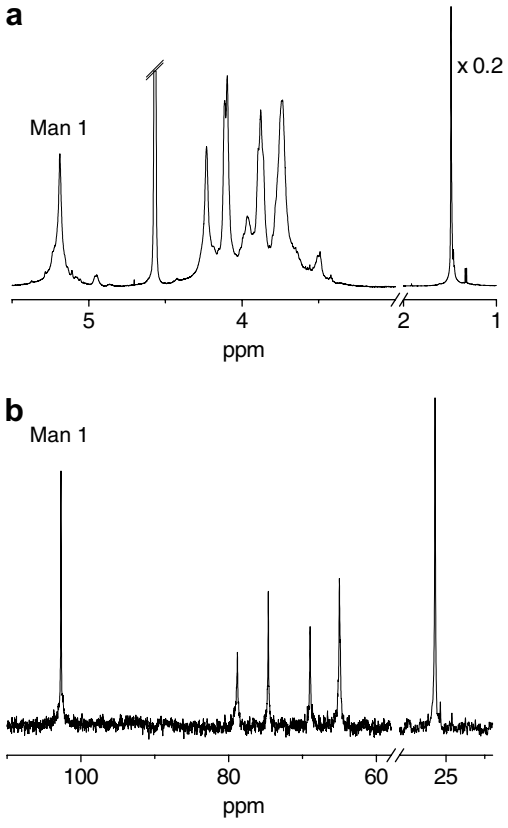

Figure 4. ^{1}H (a) and ^{13}C NMR (b) spectra of the sample **IL5-IEC** recorded at 50 °C. ×0.2 indicate that the intensity of the methyl resonances was multiplied by 0.2.

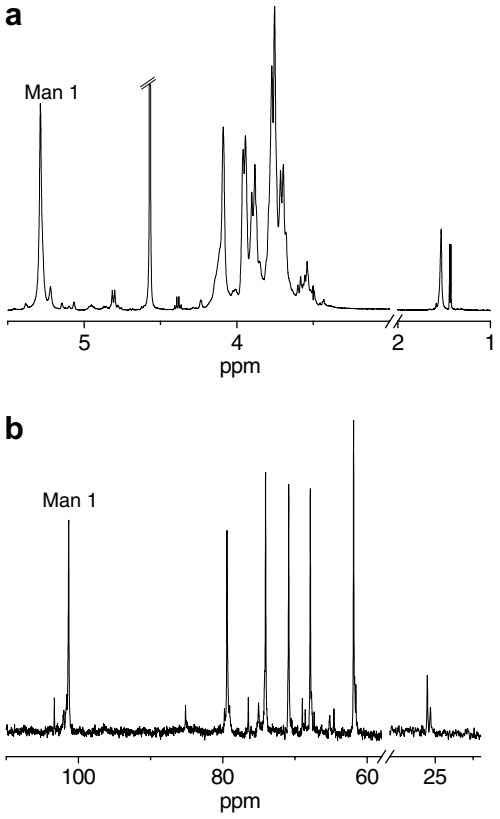

Figure 5. ^{1}H (a) and ^{13}C NMR (b) spectra of the sample **IL4-DP** recorded at 50 °C.

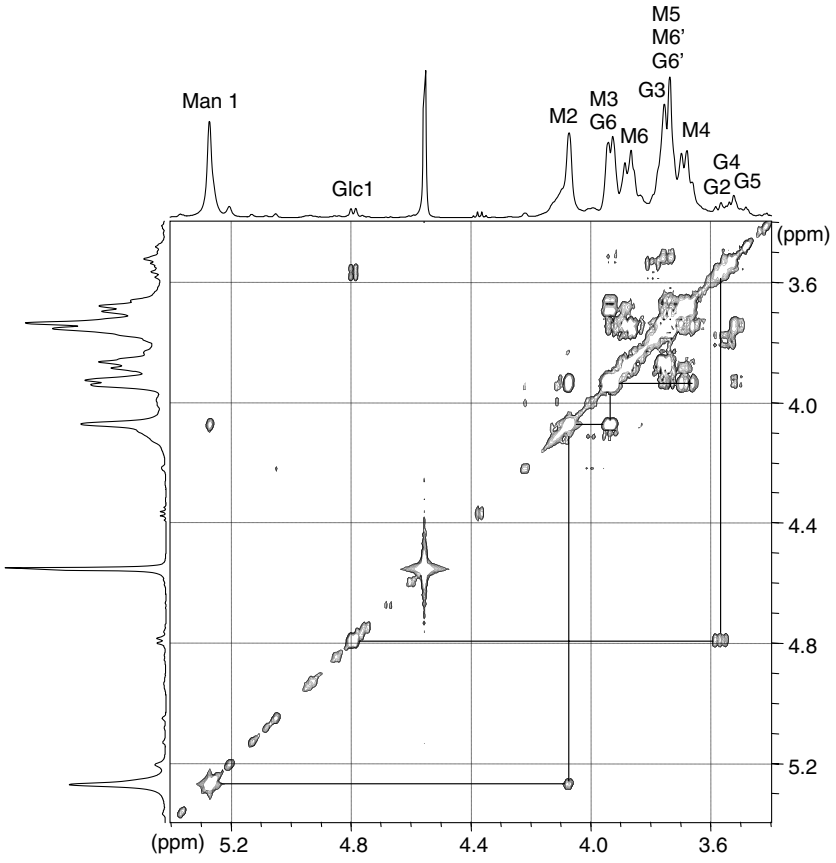

Figure 6. Part of a COSY spectrum of the sample **IL4-DP** recorded at 50 °C.

(Fig. 6), HSQC and TOCSY spectra unravelled all the polysaccharide resonances, which are reported in Table 3. The chemical shift of C-2 was consistent with a (1→2) linkage, and the carbon assignments were in good agreement with the literature data for α-(1→2)-mannan and related oligomannans.[30,31] T-ROESY and NOESY spectra (data not shown) presented further evidence of the linkage position with strong H-1/H-2 cross-peaks. The small ^{1}H and ^{13}C anomeric resonances in Figure 5a and b (at 4.79 and 103.35 ppm, respectively), together with the ^{1}H $J_{1,2}$ (7.9 Hz), were assigned to a β-anomeric signal. Inspection of the 2D NMR spectra at a low contour plot level resulted in tracing the ^{1}H and ^{13}C resonances for this residue, and they are reported in Table 3. These data showed an excellent agreement with published oligoglucans chemical shifts,[32] and established that the minor component of **IL4-DP** is a β-(1→3)-glucan. In addition, the very high Man to Glc ratio in **IL4-DP** indicated an extensive degradation of the glucan polymer.

3.7. Occurrence of simultaneous depyruvylation and EPS degradation by treatment with oxalic acid: characterisation of the products

To evaluate the hypothesis of the acidic degradation of the glucan, the reaction with oxalic acid was repeated on **IL5** batch, recovering both the material inside (**IL5-DP**) and outside the dialysis bag (**IL5-DPE**). ^{1}H and ^{13}C NMR spectra of **IL5-DP** (data not shown) showed

Table 3. ^{1}H and ^{13}C NMR chemical shifts of **IL-DP4**

Residue	Nucleus	Chemical shift (ppm)[a]					
		1	2	3	4	5	6,6′
α-2-Man*p*	^{1}H	5.27	4.07	3.93	3.68	3.74	3.87, 3.75
	^{13}C	101.37	79.44	70.89	67.90	74.09	61.89
β-3-Glc*p*	^{1}H	4.79	3.57	3.79	3.54	3.51	3.93, 3.74
	^{13}C	103.35	74.09	85.18	68.99	76.49	n.d.

[a] Chemical shifts relative to internal acetone (2.225 ppm for ^{1}H and 31.07 ppm for ^{13}C).

that the sample differed from **IL4-DP** only for the sugars ratio (**IL4-DP**–Man/Glc 15.3:1; **IL5-DP**–Man/Glc 6.4:1), a characteristic ascribable only to the differences of Man/Glc molar ratios in the native samples **IL4** and **IL5** (Table 1), and not to a different degree of degradation. Therefore, no further characterisation was carried out. Sample **IL5-DPE** was analysed by size-exclusion chromatography on a Bio-Gel P-2 column and the elution profile is shown in Figure 7. Selected single fractions were analysed by ESIMS and the data obtained are summarised in Table 4. The mass spectra identified oligosaccharides constituted of 2, 3, 4, 5 and 6 hexoses. Fraction 54 also contained lower amounts of a trisaccharide composed of two hexoses and one 6-deoxy hexose residues; the presence of the latter monosaccharide was consistent with a low intensity signal found at about 1.33 ppm in the ^{1}H NMR spectra and at 20.13 ppm in the ^{13}C NMR spectra of native or degraded **IL4** and **IL5** samples (see for instance Fig. 5).

Fractions within individual chromatographic peak were pooled together (peak I = fractions 57–59; peak II = fractions 52–55; peak III = fractions 48–50; peak IV = fractions 44–46) as indicated in Figure 7, treated with $NaBD_4$, for reduction of the reducing end sugar residue, and subjected to methylation analysis. GLC and GLC–MS data (Table 5) showed that all peaks contained both glucose and mannose derivatives originated from the (1→3)-glucan and (1→2)-mannan EPS, and therefore indicating that treatment with oxalic acid indeed depolymerised both polysaccharides. However, the glucan was degraded more than the mannan, since glucose derivatives were more abundant than the mannose ones. This finding was in agreement with the composition of the polymer **IL5-DP** constituted mainly of mannose. The 3-substituted glucitol residue, formed by reduction of the glucose reducing ends, was present in all peaks, but never reached an equimolar ratio with the non-reducing terminal Glc (t-Glc), as expected for linear oligomers. A possible explanation resides in the partial loss of this residue during the chemical work-up due to the high volatility of alditols containing high levels of methyl substitution (the 3-glucitol residues bears five methoxyl and one acetyl groups). The 2-substituted mannitol residue, expected from reduction of the mannose reducing ends, was never detected. The lack of this derivative might be explained, besides its high volatility, with the low concentration of the mannan oligomers, since mannan polysaccharide was degraded less than the glucan one. The quantification of the data was also affected by the lack of the effective carbon-response factors in the literature for 3-substituted glucitol and 2-substituted mannitol derivatives. Despite the incomplete information of the residues at the reducing end, the relative molar ratios of the derivatives reported in Table 5 were in good agreement with the presence of homo-oligosaccharides. Moreover, the evaluation of the size of the oligosaccharides present in each peak was consistent with the ESIMS data (Table 4). The co-elution of a gluco-pentasaccharide and a manno-

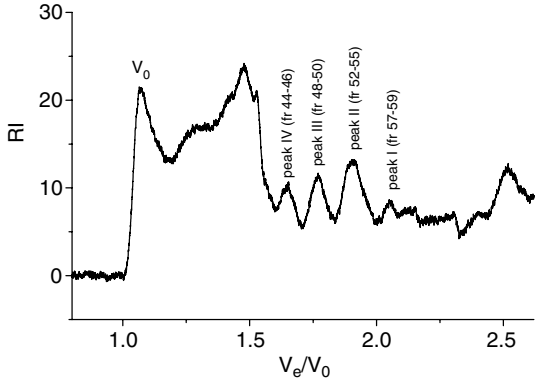

Figure 7. Elution profile of sample **IL5-DPE** from size-exclusion chromatography on a Bio-Gel P-2 column. The numbers indicate the fractions pooled together because they belong to a single peak.

Table 4. ESIMS data of single chromatographic fractions from size-exclusion chromatography of **IL5-DPE**

Fraction #	Ions *m/z*	Assignment
45	1008.6	$[Hex\text{-}Hex\text{-}Hex\text{-}Hex\text{-}Hex\text{-}Hex + NH_4]^+$
45	846.4	$[Hex\text{-}Hex\text{-}Hex\text{-}Hex\text{-}Hex + NH_4]^+$
49	684.2	$[Hex\text{-}Hex\text{-}Hex\text{-}Hex + NH_4]^+$
54	506.2	$[dHex\text{-}Hex\text{-}Hex + NH_4]^+$
54	522.2	$[Hex\text{-}Hex\text{-}Hex + NH_4]^+$
58	360.1	$[Hex\text{-}Hex + NH_4]^+$

Table 5. Methylation analysis of peaks I, II, III and IV from size-exclusion chromatography on Bio-Gel P-2 and deduced oligosaccharides size

Deduced linkage[a]	Molar ratio				
	RRT[c]	I[d]	II	III	IV
3-Glc-ol[b]	0.64	0.22	0.34	0.30	0.22
t-Man	0.97	0.10	0.39	0.39	0.26
t-Glc	1.00	1.00	1.00	1.00	1.00
3-Glc	1.18	—	1.27	2.17	3.32
2-Man	1.19	—	0.49	0.85	1.10
Oligosaccharides size[e]		2G, 2M	3G, 3M	4G, 4M	5G, 6M

[a] Deduced linkage = glycosidic linkage deduced from partially methylated alditol acetates derivatives. 3-Glc-ol = 3-*O*-acetyl-1,2,4,5,6-penta-*O*-methylglucitol; t-Man = 1,5-di-*O*-acetyl-2,3,4,6-tetra-*O*-methylmannitol; t-Glc = 1,5-di-*O*-acetyl-2,3,4,6-tetra-*O*-methylglucitol; 3-Glc = 1,3,5-tri-*O*-acetyl-2,4,6-tri-*O*-methylglucitol; 2-Man = 1,2,5-tri-*O*-acetyl-3,4,6-tri-*O*-methylmannitol.

[b] 3-Glc-ol = C-1 deuterated according to GLC–MS, derived from reducing end.

[c] RRT = retention times relative to t-Glc.

[d] I, II, III, IV = peaks from size-exclusion chromatography as reported in Figure 7.

[e] 2G = glucan disaccharide; 2M = mannan disaccharide.

hexasaccharide in peak IV might be explained taking into account that separation by size-exclusion chromatography is based on the differences in hydrodynamic volumes, which might be diverse for oligosaccharides with identical degree of polymerisation but possessing different type of glycosidic bonds. Therefore, co-elution of a β-(1→3)-linked glucose pentasaccharide with an α-(1→2)-linked mannose-hexasaccharide might happen and this behaviour will be better clarified in the discussion of the possible conformations assumed by the two polymers.

3.8. Three-dimensional models of oligosaccharides

The unusually high pyruvate substitution prompted us to look for possible conformational features of both [2)-[4,6-*O*-(1-carboxyethylidene)]-α-D-Man*p*(1→]$_n$ and [3)-[4,6-*O*-(1-carboxyethylidene)]-β-D-Glc*p*(1→]$_n$ chains. Although this modelling investigation was very preliminary, it revealed interesting characteristics of the EPS conformation (Fig. 8a and b). According to the stereochemistry dictated by the (1→2) and (1→3) glycosidic bonds, the local conformations of the two chains were both bent. However, the di-axial configuration of (1→2)-α-D-Man inter-residue linkage conferred to this molecule a more compact conformation, which could give rise to secondary structures exhibiting a rather low helical pitch. This crowded conformation was responsible for the different NMR bandwidth of Man H-1 and Glc H-1, since the geometry of the α-(1→2) glycosidic bond might lower the local chain mobility. In addition to this, the diverse local conformations of oligosaccharide chains could explain the co-elution phenomenon observed in the size-exclusion chromatography experiments, as reported above. As a matter of fact, the less bent conformation of the β-(1→3) linkage led the glucose pentasaccharide to assume a hydrodynamic volume similar to that of the α-(1→2)-linked mannose-hexasaccharide. The three-dimensional models for the mannose and glucose oligosaccharides indicated also that all the carboxyl groups were located on the outer surface of the oligomers, ready to interact with the solvent or with other molecules. Moreover, the two chains were characterised by the same amount of negative charge, but by a different charge density, a characteristic that conducted to the isolation of a sample rich in mannan by ion-exchange chromatography.

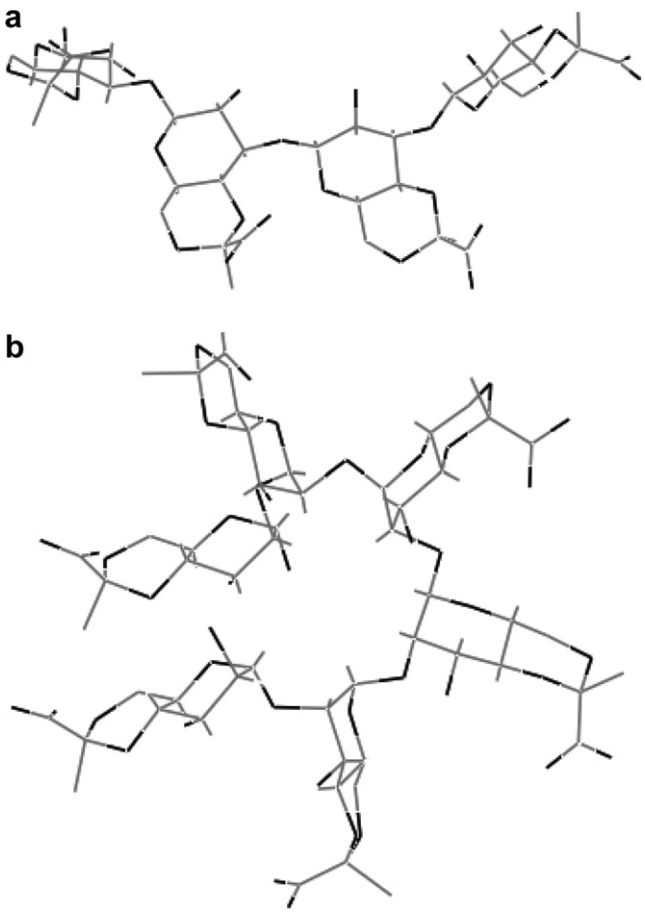

Figure 8. Local conformations of the tetrasaccharide [3)-[4,6-*O*-(1-carboxyethylidene)]-β-D-Glc*p*(1→]$_4$ (a) and of the hexasaccharide [2)-[4,6-*O*-(1-carboxyethylidene)]-α-D-Man*p*(1→]$_6$ (b).

4. Conclusion

The investigation conducted indicated that *I. limosus* produced mainly two exopolysaccharides having the following structures:

[2)-[4,6-*O*-(1-carboxyethylidene)]-α-D-Man*p*(1→]$_n$;

[3)-[4,6-*O*-(1-carboxyethylidene)]-β-D-Glc*p*(1→]$_n$

Although their very similar structure prevented their complete separation, the data collected clearly pointed to the existence of two homopolymers and not to that of a heteropolymer. In fact: (a) treatment with oxalic acid resulted in the isolation of an almost pure mannan; (b) anion-exchange chromatography of sample **IL5** led to the isolation of a fraction highly rich in mannan; (c) T-ROESY and NOESY experiments showed inter-residue connectivities within mannose rings or glucose rings, and not between mannose and glucose residues; (d) the molar ratios reported in Table 5 for the oligosaccharides were consistent with homo-oligosaccharides.

Colorimetric, composition and methylation analyses together with NMR data, also revealed small amounts of other sugars, like Gal, Rha, 3-linked Man and uronic acids, thus suggesting that the bacterium also synthesised other types of polysaccharides, but in much lower quantities.

It is worth stressing that the two polymers described here exhibit the same charge per sugar residue present in alginate, the EPS produced by *P. aeruginosa* when infecting cystic fibrosis patients. This similarity might be related to common features of the EPS produced by these two opportunistic pathogens related to lung infections. Moreover, EPS produced by the main bacteria involved in CF infections are negatively charged polymers, as many bacterial exopolysaccharides are. We were able to prove that negative charges are indeed important in the defence of bacteria against AMP of the innate immune system[11], which are generally positively charged. Ionic groups constitute the primary driving force causing interaction between EPS and AMP that impedes the bacterial membrane lysis by AMP. As reported in the literature,[11] it has to be stressed that the stability of these complexes was also dictated by specific conformational features exhibited by the different EPS.

Recently two papers pointed at additional functions of bacterial EPS. Reckseidler-Zenteno et al.[10] demonstrated that a *B. pseudomallei* mutant unable to produce its capsular polysaccharide (CPS) was more easily cleared by serum then the wild-type strain. This finding was due to the interaction of wild type CPS with C3b factor of the complement system, which inhibited its binding to the bacterial membrane, thus stimulating the events that eventually lead to the bacterial cell lysis. In fact, it is known[33] that the C3 factor binds bacterial membranes through a covalent ester bond involving polysaccharide hydroxyl groups thus contributing to the attachment of the complement factors on the bacterial cell surface.

The second paper[8] showed that EPS produced by *B. cenocepacia* inhibited neutrophil chemotaxis and scavenged reactive oxygen species thus lowering the response of the immune system to infections. It has to be noted that, similarly to *I. limosus*, the *B. cenocepacia* strain considered in the above reported investigation produced a mixture of three different polysaccharides. Therefore, investigation on whether EPS in mixtures have a synergistic effect when exerting their biological role would be valuable.

All the above reported findings indicated that bacterial EPS exhibit a variety of different activities directed to the protection of the microorganisms and the knowledge of their structural chemical motifs is key information for the investigation of the factors involved in the maintenance of the infection. In the case of *I. limosus*, it will be interesting to further pursue the structure–function relationship investigation in order to understand the role of pyruvate substitution and the reason why two similar, but not identical, EPS are produced. A possible working hypothesis is that masking the hydroxyl groups and producing more than one EPS with different conformations are both modulating factors against different antimicrobial agents or even bacterial competitors.

Acknowledgements

The authors thank Professor Peter Vandamme for the gift of the *I. limosus* strain LMG 20952^T. Dr. F. Zanetti (Eurand International SpA, Trieste, Italy) is gratefully acknowledged for the use of the Hewlett Packard 5971 mass selective detector. ESI mass spectra were run at the Centro Servizi Polivalenti di Ateneo (University of Trieste). This study was supported by a grant of the Friuli Venezia Giulia Regional Government (LR11/2003, Project No. 200502027001) and by the Italian Cystic Fibrosis Foundation. The Kathleen Foreman Casali Foundation is gratefully acknowledged for a fellowship to Y.H.

References

1. Welsh, M. J.; Tsui, L.-C.; Boat, T. F.; Beaudet, A. L. Cystic fibrosis. In *The Metabolic and Molecular Basis of Inherited Disease*; Scriver, C. R., Beaudet, A. L., Sly, W. S., Valle, D., Eds.; McGraw-Hill: New York, 1995; pp 3799–3876.
2. Coenye, T.; Goris, J.; Spilker, T.; Vandamme, P.; LiPuma, J. J. *J. Clin. Microbiol.* **2002**, *40*, 2062–2069.
3. Wellinghausen, N.; Essig, A.; Sommerburg, O. *Emerg. Infect. Dis.* **2005**, *11*, 457–459.
4. Chiron, R.; Marchandin, H.; Counil, F.; Jumas-Bilak, E.; Freydiere, A. M.; Bellon, G.; Husson, M. O.; Turck, D.; Bremont, F.; Chabanon, G.; Segonds, C. *J. Clin. Microbiol.* **2005**, *43*, 3938–3943.
5. Govan, J. R. W.; Deretic, V. *Microbiol. Rev.* **1996**, *60*, 539–574.
6. Martin, D. W.; Schurr, M. J.; Mudd, M. H.; Govan, J. R. W.; Holloway, B. W.; Deretic, V. *Proc. Natl. Acad. Sci. U.S.A.* **1993**, *90*, 8377–8381.
7. Conway, B. A.; Chu, K. K.; Bylund, J.; Altman, E.; Speert, D. P. *J. Infect. Dis.* **2004**, *190*, 957–966.
8. Bylund, J.; Burgess, L. A.; Cescutti, P.; Ernst, R. K.; Speert, D. P. *J. Biol. Chem.* **2006**, *281*, 2526–2532.
9. Pier, G. B.; Coleman, F.; Grout, M.; Franklin, M.; Ohman, D. E. *Infect. Immun.* **2001**, *69*, 1895–1901.
10. Reckseidler-Zenteno, S. L.; De Vinney, R.; Woods, D. E. *Infect. Immun.* **2005**, *73*, 1106–1115.
11. Herasimenka, Y.; Benincasa, M.; Mattiuzzo, M.; Cescutti, P.; Gennaro, R.; Rizzo, R. *Peptides* **2005**, *26*, 1127–1132.
12. Sage, A.; Linker, A.; Evans, L. R.; Lessie, T. G. *Curr. Microbiol.* **1990**, *20*, 191–198.
13. Dubois, M.; Gilles, K. A.; Hamilton, J. K.; Rebers, P. A.; Smith, F. *Anal. Chem.* **1956**, *28*, 350–356.
14. Blumenkrantz, N.; Asboe-Hansen, G. *Anal. Biochem.* **1973**, *54*, 484–489.
15. Anthon, G. E.; Barrett, D. M. *J. Sci. Food Agric.* **2003**, *83*, 1210–1213.
16. Albersheim, P.; Nevins, D. J.; English, P. D.; Karr, A. *Carbohydr. Res.* **1967**, *5*, 340–345.
17. Dudman, W. E.; Franzén, L.-E.; Darvill, J. E.; McNeil, M.; Darvill, A. G.; Albersheim, P. *Carbohydr. Res.* **1983**, *117*, 141–156.
18. Gerwig, G. J.; Kamerling, J. P.; Vliegenthart, J. F. G. *Carbohydr. Res.* **1978**, *62*, 349–357.
19. Gerwig, G. J.; Kamerling, J. P.; Vliegenthart, J. F. G. *Carbohydr. Res.* **1979**, *77*, 1–7.
20. Hakomori, S. *J. Biochem. (Tokyo)* **1964**, *55*, 205–208.

21. Phillips, L. R.; Fraser, B. A. *Carbohydr. Res.* **1981**, *90*, 149–152.
22. Dell, A. *Methods Enzymol.* **1990**, *193*, 647–660.
23. Sweet, D. P.; Shapiro, R. H.; Albersheim, P. *Carbohydr. Res.* **1975**, *40*, 217–225.
24. Wang, Y.; Hollingsworth, R. I.; Kasper, D. L. *Carbohydr. Res.* **1999**, *319*, 141–147.
25. Osman, S. F.; Fett, W. F. *J. Bacteriol.* **1989**, *171*, 1760–1762.
26. Hashimoto, W.; Nankai, H.; Mikami, B.; Murata, K. *J. Biol. Chem.* **2003**, *278*, 7663–7673.
27. Garegg, P. J.; Jansson, P.-E.; Lindberg, B.; Lindh, F.; Lonngren, J.; Kvarnström, I.; Wolfgang, N. *Carbohydr. Res.* **1980**, *78*, 127–132.
28. Baumann, H.; Tzianabos, A. O.; Brisson, J.-R.; Kasper, D. L.; Jennings, H. J. *Biochemistry* **1992**, *31*, 4081–4089.
29. Bock, K.; Lundt, I.; Pedersen, C. *Tetrahedron Lett.* **1973**, *13*, 1037–1040.
30. Bock, K.; Pedersen, C.; Pedersen, H. *Adv. Carbohydr. Chem. Biochem.* **1984**, *42*, 193–225.
31. Petersen, B. O.; Krah, M.; Duus, J. Ø.; Thomsen, K. K. *Eur. J. Biochem.* **2000**, *267*, 361–369.
32. Grimmecke, H. D.; Voges, M.; Knirel, Y. A.; Shashkov, A. S.; Lauk, W.; Kiesel, B. *Carbohydr. Res.* **1994**, *253*, 283–286.
33. Hostetter, M. K.; Thomas, M. L.; Rosen, F. S.; Tack, B. F. *Nature* **1982**, *298*, 72–74.